Supplementary Material for

THE RNA TRANSPORT ELEMENT OF THE MURINE MusD RETROTRANSPOSON REQUIRES LONG-RANGE INTRAMOLECULAR INTERACTIONS FOR FUNCTION

Michal Legiewicz, Andrei S. Zolotukhin, Guy R. Pilkington, Katarzyna J. Purzycka, , Michelle Mitchell, Hiroaki Uranishi, Jenifer Bear, George N. Pavlakis, Stuart F.J. Le Grice and Barbara K. Felber

Figure Legends

Supplementary Figure 1: Chemical Probing of MTE RNA via SHAPE. SHAPE reactivity histogram of the ~400 nt MTE RNA. Red and orange notations are expected to fall in single-stranded regions, while bases indicated in black and blue correspond predominantly to either double-stranded regions or tertiary interactions.

Supplementary Figure 2: Chemical probing (SHAPE) of MTE variants with altered kissing loops. Difference plots of 1M7 reactivity between MTE mutant (red) and wt RNA (blue) are shown. (A-D**)** analysis of mutants m2-m5, respectively. In each case entire MTE RNA length was analyzed and positions in range of 56-220 are plotted and *L3* and *IL8* regions are marked with dashed boxes in the plot.

Supplementary Figure 3: Interrogation of the MTE kissing loops with aiSHAPE. **(**A) Effect of hybridizing 1B oligonucleotide (orange font) to the *IL8* loop on chemical reactivity of *L3* nucleotides. Residues exhibiting enhanced reactivity are indicated by shaded squares. DNA and LNA positions within antisense oligonucleotide are in lower or upper case, respectively. (B**)** Plot of 1M7 reactivity of native (blue trace) and antisense-interfered MTE RNA (orange trace). 1M7 reactivity profiles were derived for the entire 412 nt MTE, indicating that all structural changes were restricted to the kissing interaction partners. Hybridizing an antisense chimera 1B complementary to *IL8* significantly enhanced 1M7 reactivity within the complementary positions of *L3* loop (C83, U84 and A86-A89). Confirmation that 1B was stably bound to *IL8* was evident from a major pause site it induced in the reverse transcription step.

Supplementary Figure 4: Chemical probing (SHAPE) of MTE variants with altered pseudoknot domain. Difference plots of 1M7 reactivity between MTE mutant (orange) and wt RNA (blue) are shown. A-C analysis of mutants m7, m8 and m6, respectively. In each case entire MTE RNA length was analyzed and appropriate pseudoknot regions are marked with dashed boxes in the plot.

Supplementary Figure 5: Analysis of Isolated Pseudoknots of MTE wt and Mutant m6. (A) and (B) Secondary structure models based on SHAPE-constraining folding of the isolated pseudoknot domains of native sequence (wt) and mutant m6 MTE, respectively. Color-coding corresponds to 1M7 reactivity level; <0.2, black; 0.2-0.5, blue; 0.5-0.8, orange; >0.8, red; gray – no data. Introduced interactions *IIA/IIB* and/or *IIIA/IIIB* are represented by purple and green lines, respectively. Significant differences in the 1M7 reactivity between isolated pseudoknots and pseudoknots in the sequence context of the full length MTEs are indicated by arrows and do not introduce changes into structural models of RNA pseudoknots. (C**)** mobility of MTE wt and m6 short constructs on native 4% TBM gel.

Supplementary Figure 1:

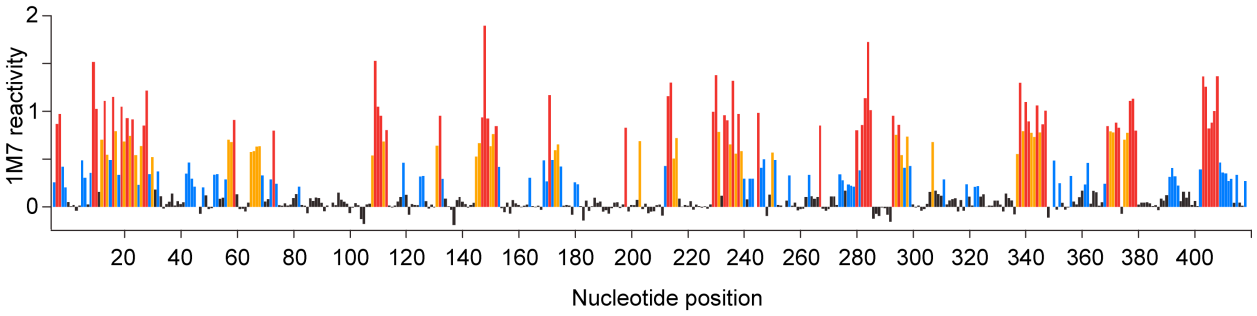

Supplementary Figure 2:

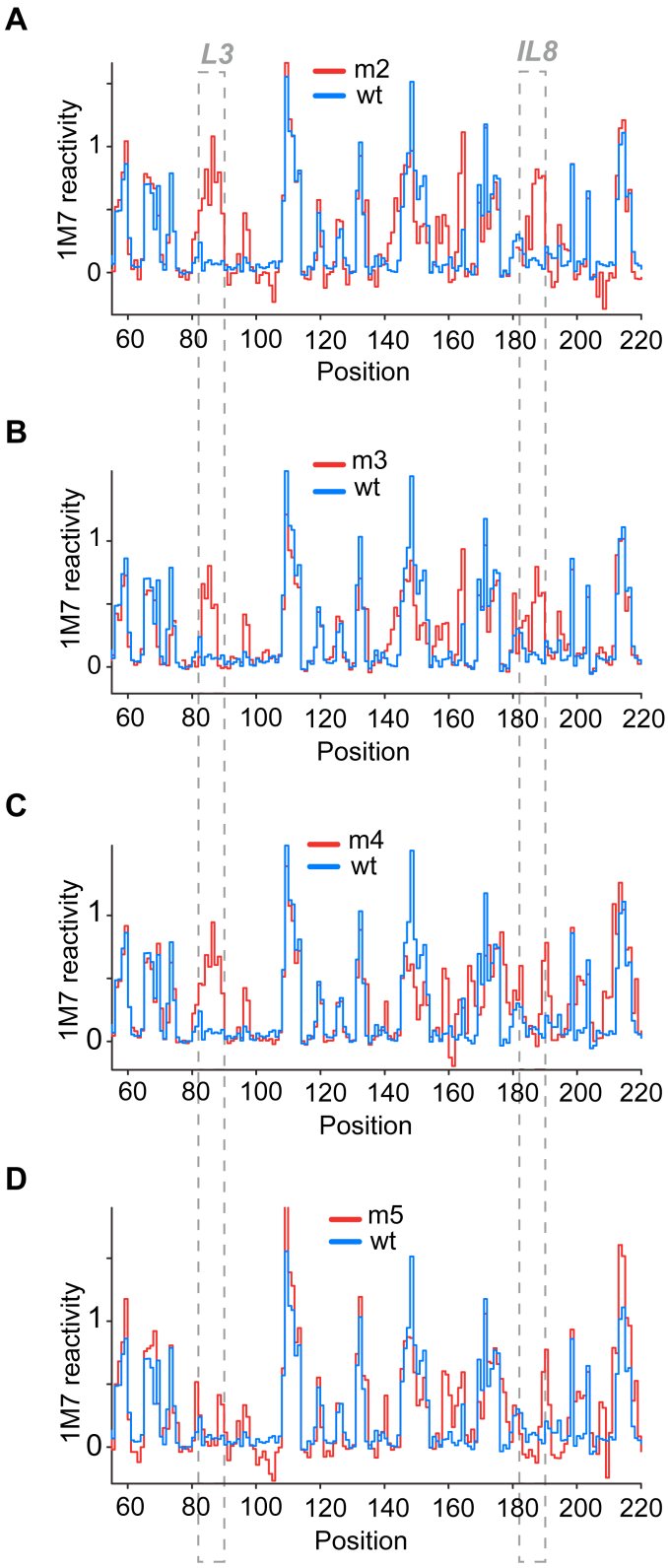

Supplementary Figure 3:

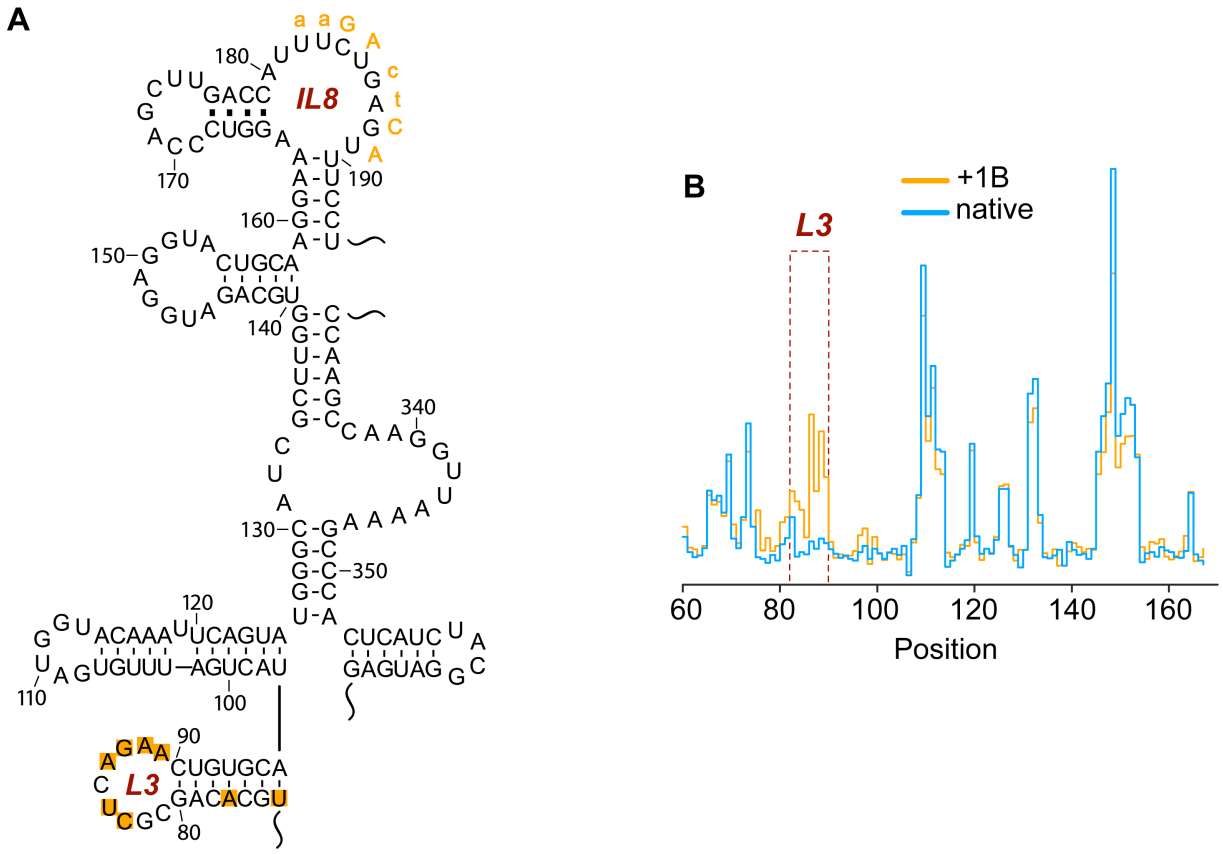

Supplementary Figure 4:

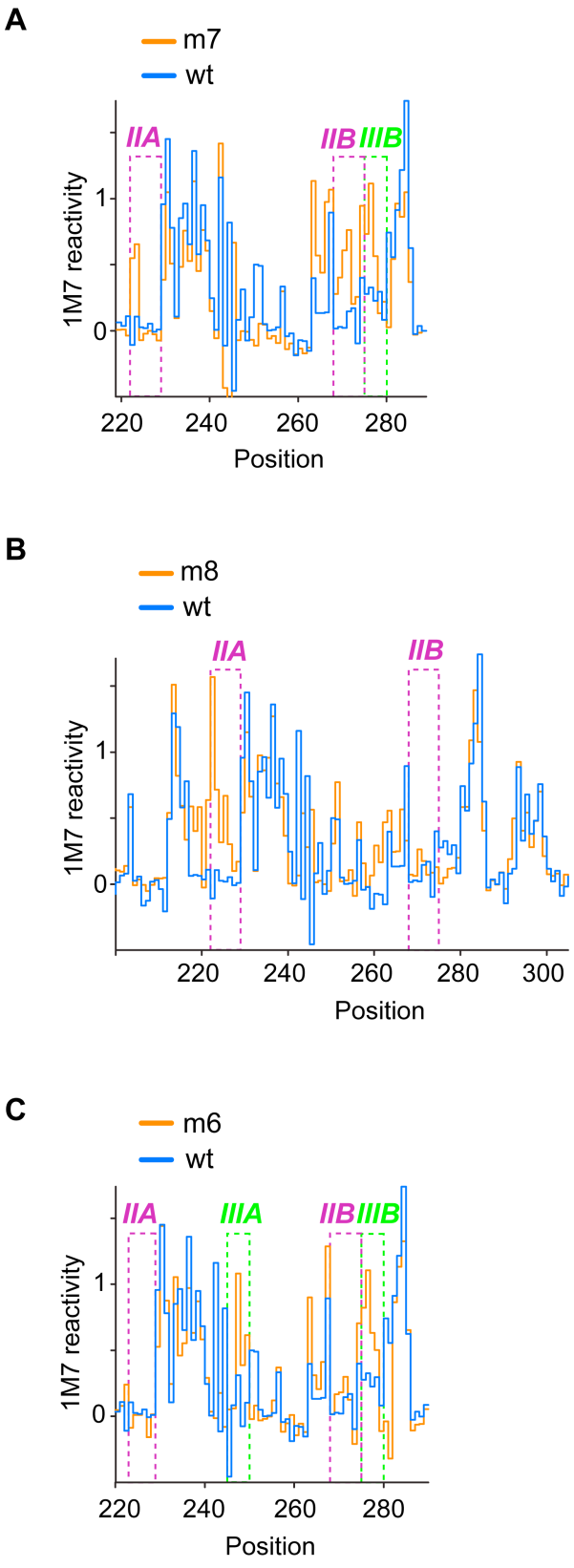

Supplementary Figure 5:

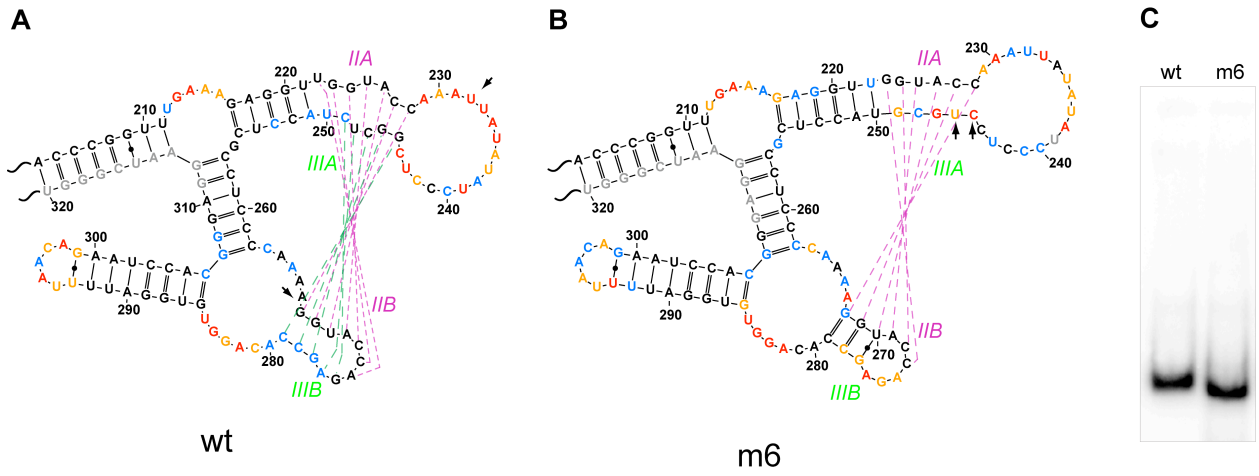

Supplementary Table 1. Antisense Oligonucleotides used for ai-SHAPE

Antisense Oligonucleotide	Sequence	Chemical composition
1B	5′-**ACTCAGAA**-3′	LNA/DNA
3A	5′-**GAGCC**-3′	LNA/DNA
3B	5′-**GGCTC**-3′	LNA/DNA
2B	5′-**GGCUCUGGUA**-3′	2′-*O*-methyl RNA
4	5′-**GAGGGAU**-3′	2′-*O*-methyl RNA
6	5′-**CCUGUGGCUC**-3′	2′-*O*-methyl RNA